Toxicology Letters 394 (2024) 1–10

Contents lists available at ScienceDirect

Toxicology Letters

journal homepage: www.journals.elsevier.com/toxicology-letters

Combined *in vitro* and *in silico* mechanistic approach to explore the potential of *Alternaria* mycotoxins alternariol and altertoxin II to hamper γH2AX formation in DNA damage signaling pathways

Francesco Crudo [a], Luca Dellafiora [b], Chenyifan Hong [a], Lena Burger [a], Maximilian Jobst [a,c,d], Giorgia Del Favero [a,c], Doris Marko [a,c,*]

[a] Department of Food Chemistry and Toxicology, Faculty of Chemistry, University of Vienna, Währinger Str. 38, Vienna 1090, Austria
[b] Department of Food and Drug, University of Parma, Area Parco delle Scienze 27/A, Parma 43124, Italy
[c] Core Facility Multimodal Imaging, Faculty of Chemistry, University of Vienna, Währinger Str. 42, Vienna 1090, Austria
[d] University of Vienna, Vienna Doctoral School in Chemistry (DoSChem), Währinger Str. 42, Vienna 1090, Austria

ARTICLE INFO

Keywords:
Alternaria mycotoxins
γH2AX
Doxorubicin
DNA damage
Kinase inhibition

ABSTRACT

Risk assessment of food and environmental contaminants is faced by substantial data gaps and novel strategies are needed to support science-based regulatory actions. The *Alternaria* mycotoxins alternariol (AOH) and altertoxin II (ATXII) have garnered attention for their possible genotoxic effects. Nevertheless, data currently available are rather scattered, hindering a comprehensive hazard characterization. This study combined *in vitro*/*in silico* approaches to elucidate the potential of AOH and ATXII to induce double-strand breaks (DSBs) in HepG2 cells. Furthermore, it examines the impact of co-exposure to AOH and the DSB-inducing drug doxorubicin (Doxo) on γH2AX expression. AOH slightly increased γH2AX expression, whereas ATXII did not elicit this response. Interestingly, AOH suppressed Doxo-induced γH2AX expression, despite evidence of increased DNA damage in the comet assay. Building on these observations, AOH was postulated to inhibit γH2AX-forming kinases. Along this line, *in silico* analysis supported AOH potential interaction with the ATP-binding sites of these kinases and immunofluorescence experiments showed decreased intracellular phosphorylation events. Similarly, *in silico* results suggested that ATXII might also interact with these kinases. This study emphasizes the importance of understanding the implications of AOH-induced γH2AX expression inhibition on DNA repair processes and underscores the need for caution when interpreting γH2AX assay results.

1. Introduction

Alternaria fungi are known producers of a wide variety of structurally different mycotoxins, some of which raise concerns due to potential health impacts on both humans and animals. Among these mycotoxins, alternariol (AOH) and altertoxin II (ATXII) have garnered attention for their genotoxic properties. AOH has been found to contaminate various foods, including tomatoes, grains, sunflower seeds, fruits, and their respective products (EFSA, 2011). Conversely, data on the occurrence of ATXII remain limited, with previous reports primarily indicating apples and dried grape berries as potential sources (Mikušová et al., 2014; Puntscher et al., 2020).

The dibenzo-α-pyrone AOH has been associated with various forms of DNA damage, including single-strand breaks (SSB), double-strand breaks (DSB), and oxidative DNA damage (Fernández-Blanco et al., 2015; Fleck et al., 2016; Tiessen et al., 2017). Although not fully elucidated, AOH seems to exert its genotoxic effects through various mechanisms, including, for instance, the generation of reactive oxygen species and the poisoning of DNA topoisomerase (TOPO), particularly the IIα isoform (Fehr et al., 2009; Solhaug et al., 2012). TOPOs represent a group of enzymes responsible for controlling the topological structure of DNA by introducing single (TOPO I) or double (TOPO II) strand breaks, which, within the catalytic cycle of the enzyme, are subsequently repaired through rejoining processes. The poisoning of TOPOs consists in the compound-dependent stabilization of the transient covalent DNA-topoisomerase complex, thus interfering with the important

Abbreviations: AOH, alternariol; ATXII, altertoxin II; Doxo, doxorubicin; DSBs, double-strand breaks; SSBs, single-strand breaks.

* Correspondence to: Department of Food Chemistry and Toxicology, University of Vienna, Währinger Str. 38, Wien 1090, Austria.
E-mail address: doris.marko@univie.ac.at (D. Marko).

https://doi.org/10.1016/j.toxlet.2024.02.008
Received 19 October 2023; Received in revised form 6 February 2024; Accepted 21 February 2024
Available online 23 February 2024

topology-regulating activity of TOPOs during DNA replication or transcription. TOPO-poisoning not only traps the enzyme in the covalent link at the DNA but also prevents the rejoining of DNA strands, resulting in the persistence of SSBs (in the case of TOPO I poisoning) and DSBs (in the case of TOPO II poisoning) (Pommier, 2013). It is believed that poisoning of TOPO II primarily accounts for the DSB properties associated with AOH (Fleck et al., 2016). Genotoxicity of AOH has been linked to mutational properties as exemplified in the hypoxanthine-guanine phosphoribosyl transferase (V79 cells) and thymidine kinase assays (mouse lymphoma cells) (Fleck et al., 2016), as well as by increase in *Salmonella typhimurium* TA100 revertants in the Ames test (Schrader et al., 2001; Crudo et al., 2023). Despite limited data for the perylene quinone ATXII, it has been found to induce DNA strand breaks (Aichinger et al., 2022; Fleck et al., 2012; Schwarz et al., 2012) and mutations (Fleck et al., 2012) more potently than AOH. Of note, ATXII can form covalent adducts with DNA thanks to the presence of an epoxide group in its chemical structure (Soukup et al., 2020), and it can act as a catalytic inhibitor of TOPO II (Fleck et al., 2016; Tiessen et al., 2013).

Despite these insights, the available data regarding the *Alternaria* mycotoxins AOH and ATXII remains insufficient for a comprehensive risk assessment. It is important to highlight that a preliminary assessment conducted by the European Food Safety Authority (EFSA) concerning the risk associated with AOH exposure has revealed that the mean exposure at the 95th percentile could exceed the threshold of toxicological concern (TTC) for genotoxic compounds (EFSA, 2011). This underscores the pressing need for additional data and research on this mycotoxin. In the context of food safety, several steps are currently made to develop and enforce new approach methodologies (NAMs) for data collection and, where possible, reduce the use of animals for experimental needs in favor of *in vitro* and *in silico* approaches (Cattaneo et al., 2023).

In this context, different *in vitro* test methods are routinely employed for evaluating the genotoxic properties of chemicals, with the comet assay being a prominent choice for assessing DNA damage at the individual cell level. The comet assay is widely acknowledged as a 'gold standard' in genotoxicity studies for its ability to reliably detect various forms of DNA damage, including SSBs, double-strand breaks DSBs, and alkali-labile sites, depending on the specific assay conditions applied (Collins, 2004). Despite its notable advantages, such as sensitivity, cost-effectiveness, and the ability to assess diverse types of DNA damage, this assay has limitations related to its time-consuming nature, making it unsuitable for high-throughput screening.

As a response to this limitation, researchers globally have focused on developing high-throughput genotoxicity tests, such as the In-cell Western assay of γH2AX (Kopp et al., 2019). This assay indirectly detects DNA DSBs through the quantification of the phosphorylated histone γH2AX, whose production occurs in response to DSBs. In particular, γH2AX foci, which develop around DSB sites thanks to the action of kinases like Ataxia Telangiectasia Mutated (ATM), Ataxia Telangiectasia and Rad3-related (ATR), and DNA-dependent Protein Kinase (DNA-PKc), actively participate in recruiting repair proteins to initiate and facilitate DNA repair mechanisms (Mah et al., 2010). Quantification of the γH2AX can be performed with a wide variety of different techniques, such as high-content analysis, western blot, immunofluorescence microscopy and mass spectrometry (Kopp et al., 2019). Furthermore, this assay is applicable to various cell lines, including, for instance, the widely used HepG2 cell line, which has previously demonstrated a reliable correlation between γH2AX expression and DNA double-strand breaks (Wahyuni et al., 2022). Despite the advantage of the γH2AX assay of being a high-throughput assay, it indirectly quantifies DSBs, making it susceptible to potential misinterpretation of the results.

Taking these as starting points, the primary objective of this study was to investigate the potential of *Alternaria* mycotoxins AOH and ATXII to induce DSBs in DNA. We quantified γH2AX expression levels induced by both mycotoxins and assessed the impact of AOH on γH2AX expression during co-exposure of the hepatocellular carcinoma HepG2 cell line to AOH and the DSB-inducing chemotherapeutic drug doxorubicin (Doxo). *In vitro* experiments were complemented by *in silico* analyses, to delve into the underlying mechanisms governing the observed changes in γH2AX expression.

2. Materials and methods

2.1. Materials

For cell culture experiments, Roswell Park Memorial Institute (RPMI) 1640 medium, heat-inactivated fetal bovine serum (FBS), and penicillin/streptomycin (P/S) solution were purchased from GIBCO Invitrogen™ Life Technologies (Karlsruhe, Germany). The hepatocellular carcinoma HepG2 cell line was obtained from the European Collection of Authenticated Cell Cultures (Wiltshire, United Kingdom). AOH (from *Alternaria* sp.) and doxorubicin hydrochloride were purchased from Sigma-Aldrich (St. Louis, USA), while ATXII was previously purified in-house from an *Alternaria alternata* DSM 62010 culture grown on rice (Puntscher et al., 2019). The CellTiter-Blue® Cell Viability reagent was acquired from Promega Corporation (Fitchburg, USA). Anti-phospho-Histone H2A.X (Ser139) Antibody (clone JBW301) was purchased from Sigma-Aldrich Corporation (St. Louis, USA), while Alexa Fluor™ 633 F(ab')2 fragment of goat anti-mouse IgG (H+L), Bovine Serum Albumin (BSA; Standard Grade Powder, Fraction V), Alexa Fluor™ Phosphoserine/threonine/tyrosine polyclonal antibody (Catalog nr. 61–8300), Alexa Fluor™ donkey anti-rabbit IgG (H+L), and Invitrogen Oregon Green™ 488 phalloidin were acquired from Thermo Fisher Scientific (Germany). Fluoroshield ™ with DAPI was purchased from Sigma-Aldrich Corporation (St. Louis, USA).

2.2. Cell culture and incubation conditions

The human hepatocellular carcinoma HepG2 cell line was employed for all experiments. Cells were maintained in RPMI 1640 medium supplemented with 1 % penicillin (10,000 Units/mL)/streptomycin (10,000 μg/mL) solution and 10 % (v/v) FBS. Cells were passaged twice per week (70–80% confluency), grown at +37 °C and 5% CO_2 in a humidified incubator, and routinely screened for mycoplasma contamination.

For the experiments aiming at assessing the impact of AOH on the genotoxicity and cytotoxicity of Doxo, cell treatments were performed following the schema reported in Fig. 1. In particular, cells were pre-incubated for 1 h (time point "−1 h") with 5/50 μM AOH or 0.5% DMSO, depending on the test condition. The choice to pre-incubate the cells with AOH for 1 h before exposing them to Doxo was made with the intention of giving AOH the opportunity to reach its intracellular target (s) and potentially inhibit the kinases prior to the application of Doxo. At the end of the pre-incubation time (time point 0 h), the various test media were replaced with test media containing 0.5% DMSO, 2.5 μM Doxo, 5/50 μM AOH, or combinations of Doxo and AOH. After 2 h of treatment (timepoint 2 h), media were replaced with test media only containing 5/50 μM AOH or 0.5% DMSO, depending on the treatment. Cells were therefore incubated for additional 2 h (time point 4 h) and 20 h (timepoint 24 h). Thus, the various endpoints were assessed at multiple timepoints (−1 h, 0 h, 2 h, 4 h, and 24 h) in order to monitor their changes over time. The final DMSO concentration was 0.5% in all test conditions, which were tested in at least three biological replicates. Due to the scarce availability of ATXII, which was in-house purified, ATXII was not tested in experiments requiring the co-incubation with Doxo.

2.3. γH2AX assay

The double-strand breaks properties of the various test conditions were assessed in the HepG2 cell line by quantifying the phosphorylated

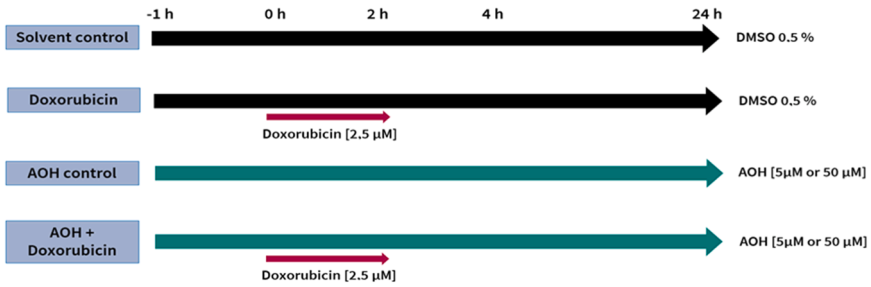

Fig. 1. Graphical representation of the incubation conditions applied to assess the ability of AOH to suppress the Doxo-induced γH2AX expression.

histone γH2AX through immunofluorescence microscopy. The quantification was performed according to Ebmeyer et al. (Ebmeyer et al., 2019), with some modifications. Briefly, 50,000 cells/well were seeded into 96-well plates (Black plate, clear bottom; Corning Incorporated, Kennebunk, USA) and grown for 24 h at 37°C and 5 % CO_2. After incubation of cells with AOH (0.1, 10, 50, and 100 µM; 4 h), ATXII (0.1, 1, 5, 12.5 µM; 4 h), or the various test conditions described in *Section 2.2* ., cells were fixed at 4°C for 20 min by addition of ice-cold methanol (50 µL/well). Thus, cells were washed thrice with PBS-T (PBS + 0.1% Tween® 20) and blocked for 1 h with 1% BSA in PBS-T (room temperature–RT; with shaking). After one washing step with PBS-T and incubation overnight at 4°C with the primary antibody solution (Anti-phospho-Histone H2A.X Antibody; 1:400 in blocking solution; 100 µL/well), cells were washed thrice with PBS-T and incubated for 1 h at RT with 100 µL/well of the secondary antibody solution (Alexa Fluor™ 633 F(ab')2 fragment of goat anti-mouse IgG; 1:500 in blocking solution). Cell nuclei were stained for 30 min with 50 µL/well of 3 µM DAPI solution (RT), followed by three washing steps with PBS-T and storage at 4°C until the time of analysis. To assess the induction of γH2AX expression, two pictures per well were acquired at wavelengths 380/460 nm (ex/em; for DAPI) and 620/655 nm (ex/em; for γH2AX) by using a Lionheart FX automated microscope equipped with the software Gen5 (ver. 3.08; BioTek Instruments Inc., Winooski, VT, USA). For each picture, at least 120 cells were automatically scored and results expressed as the mean value of the γH2AX signal intensity per cell (normalized against the solvent control). All conditions were tested in three technical replicates in at least three independent experiments, resulting in the evaluation of more than 700 cells/condition (an example of the distribution of the number of cells per optical field can be found in supplementary Figure S1). DMSO (0.5%) and Doxo (2.5 µM) were used as solvent and positive controls, respectively.

2.4. Alkaline comet assay

To assess the genotoxic effects of AOH and Doxo as single compounds and in combination, the alkaline comet assay was carried out according to (Tice et al., 2000), with slight modifications. Briefly, 350,000 cells were seeded in 3.5 cm (Ø) Petri dishes and grown at +37 ℃ and 5% CO_2 for 48 h. After exposure of cells to the various test conditions (see *Section 2.2*) for 5 h (1 h pre-incubation + 4 h; timepoint 4 h), a positive control was prepared by exposing cells treated with 0.5% DMSO to UV-B radiation for 1 min. Afterwards, each Petri dish was washed twice with PBS and cells singularized by addition of 250 µL of trypsin. After addition of 500 µL of complete growth medium, two aliquots of 30,000 cells for each sample were centrifuged at 420 rcf (10 min) and resuspended in 0.8% low-melting agarose. Cells were therefore embedded on object slides and lysed overnight (+4 ℃) by immersing the slides in a buffer containing DMSO, Triton X100, and N-lauryl sarcosine. Before the electrophoresis, slides were allowed to equilibrate for 20 min in an alkaline buffer (pH > 13) to allow the unwinding of the double helix. Electrophoresis was performed under alkaline conditions at 300 mA and 25 V for 20 min. Afterwards, the slides were washed three times with a neutralization buffer, followed by staining of the DNA with a 20 µg/mL ethidium bromide solution. Through the use of a fluorescence microscope (Zeiss Axioskop; ex = 546 ± 1 nm; em = 590 nm) and the "Comet Assay IV" software (Perceptive Instruments, Suffolk, UK), the DNA damage was assessed by measuring the tail intensity of 100 cells per object slide. Every condition was tested in at least three biological replicates. To avoid misinterpretation of the results due to cytotoxicity, cell viability was assessed by applying the CellTiter-Blue™ assay (see Section 2.5).

2.5. CellTiter-Blue™ (CTB) assay

To assess the viability of HepG2 cells after exposure to the various test conditions, the CTB assay was performed as followed. At the end of the incubation time, the medium from each well was replaced with 100 µL of CTB solution diluted 1:10 with phenol-red free DMEM. Cells were incubated for 40 min at +37°C and 5% CO2, followed by transfer of the supernatants into black 96-well plates. Fluorescence signal was measured at 590 nm through the use of a Cytation 3 imaging reader (microplate reader; BioTek, USA). The various test conditions were tested in three technical replicates and in 3 independent experiments. Results were expressed as mean fluorescence value of 3 biological replicates after normalization to the solvent control (0.5 % DMSO).

2.6. Assessment of intracellular phosphorylation status by fluorescence microscopy

To verify the ability of AOH to suppress intracellular phosphorylation processes, phosphorylated amino acids (phosphoserine/threonine/tyrosine) were quantified into the nucleus and cytoplasm by immunofluorescence microscopy according to a previously discussed procedure for acetylation, with some modifications (Jobst et al., 2023). In particular, HepG2 cells were seeded in 96-well plates (Black plate, clear bottom; Corning Incorporated, Kennebunk, USA) and incubated for 24 h at +37 ° C and 5 % CO_2. After treatment with AOH (1, 5, and 10 µM; time points 4 h or 24 h; see *Section 2.2* .), Doxo (2.5 µM), or their combinations, the cells were fixed with formaldehyde (3.7 % in PBS-A; 100 µL/well) at RT for 25 min (in the dark). The cells were washed once each with PBS-A, PBS-A-Glycin (0.363 g Glycin in 50 mL PBS-A), and PBS-A. To permeabilize the membrane, 0.2 % Triton-X in PBS-A (100 µL/well) was added and incubated at RT for 10 min (with shaking). Thereafter, the blocking solution (1 % bovine serum albumin in PBS-A) was added and cells incubated at RT for 1 h (with shaking). After removing the blocking solution, 100 µL/well of the primary antibody solution was added (Alexa Fluor™ Phosphoserine/threonine/tyrosine polyclonal antibody; Catalog nr. 61–8300; 1:1000 dilution in blocking solution) and incubated overnight at +4 ° C. Cells were washed thrice with 0.05 % Triton-X in PBS-A (10 min incubation; with shaking) and twice with PBS-A (5 min incubation; with shaking). 100 µL of a solution containing phalloidin (for the staining of the cytoskeleton; F-actin) and the secondary antibody (Invitrogen Oregon Green™ 488 phalloidin; Alexa Fluor™ donkey anti-rabbit IgG (H+L); both 1:1000 in blocking solution) was added to each well and incubated for 2 h (without shaking; in the dark). The solution was removed and the cells were washed thrice with

0.05 % Triton-X in PBS-A (10 min of incubation each, with shaking). After two additional washing steps with PBS-A (5 min of incubation, with shaking), 1 drop of a mounting medium containing DAPI (Fluoroshield ™ with DAPI) was added to each well to stain the nuclei. The fluorescence intensity was measured using a Lionheart FX automated microscope supplied with the Gen5 software (version 3.08, BioTek Instruments Inc., Winooski, VT, USA). At least two pictures per well were acquired at wavelengths 380/460 nm (ex/em; for DAPI), 620/655 (ex/em; for phosphoserine/threonine/tyrosine) and 488/509 nm (ex/em; for phalloidin). For each picture, the nuclear phosphoserine/threonine/tyrosine florescence intensities of at least 150 cells were automatically acquired by using the DAPI signal for the identification of the area occupied by the nucleus. The quantification of the cytoplasmic phosphoserine/threonine/tyrosine florescence intensity was performed in the perinuclear area (calculated automatically as a 4 μm width starting from the nucleus). All conditions were tested in three technical replicates in at least three independent experiments. DMSO (0.5 %) was used as solvent control.

2.7. In silico analysis

The model for human serine-protein kinase ATM (UniProt ID Q13315), DNA-dependent protein kinase catalytic (DNA-PKcs; UniProt ID p78527) and serine/threonine-protein kinase ATR (UniProt ID Q13535) was derived from EM structures derived from the Protein Data Bank (https://www.rcsb.org; PDB) (Burley et al., 2023) as following. The model for serine-protein kinase ATM was derived from the EM PDB structure with code 5NP0 (Cohen-Khait et al., 2017), focusing the analysis at the ATP binding site as per UniProt specifications (i.e. residues 2693–2697, 2699, 2715, 2717, 2755, 2767–2770, 2870, 2874–2875, 2877, and 2888–2889; CDD id 270715). The model for DNA-PKcs was derived from the PDB EM structure with code 7LT3 (Chen et al., 2021), focusing the analysis at the ATP binding site as per UniProt specifications (i.e. residues 3729–3733, 3735, 3751, 3753, 3791, 3803–3806, 3922, 3926–3927, 3929, 3940–3941; CDD id 270716). The model for serine/threonine-protein kinase ATR was derived from the PDB EM structure with code 5YZ0 (Rao et al., 2018), focusing the analysis at the ATP binding site as per UniProt specifications (i.e. residues 2303, 2305–2307, 2309, 2325, 2327, 2330, 2365, 2377–2380, 2385, 2480, 2482, 2493–2494; CDD id 270625). The interaction of AOH and ATX-II with the kinases mentioned above has been investigated through docking simulation in agreement with previous studies (Aichinger et al., 2020). Briefly, docking simulations were done using the software GOLD (Genetic Optimization for Ligand Docking; version 2021.1), setting the space available to arrange ligands in a 10 Å radius sphere around each pocket centroid, as it previously succeeded in providing reliable architectures of binding and in predicting the activity of compounds of toxicological concern (Aichinger et al., 2020; Maldonado-Rojas and Olivero-Verbel, 2011). Docking protocol was set according to previous studies keeping ligands fully flexible (i.e. all the routable bonds were set free to rotate) and protein semi-flexible allowing polar hydrogens free to rotate (Aichinger et al., 2020; Crudo et al., 2022). For each ligand, 10 poses were generated and scored using the internal scoring function GOLDScore, as it has been optimized for the prediction of ligand binding positions, according to the manufacturer declaration (https://www.ccdc.cam.ac.uk). Considering that the scoring assignment is proportional to the ligand-pocket fitting (the higher the score, the higher the match to the pocket's physico-chemical properties), only the best scored pose for each docked ligand was considered for the analysis, in agreement with previous studies (Aichinger et al., 2020).

2.8. Statistical analysis

All statistical analyses were performed with Microsoft Excel (v. 2308) or Origin Pro 2022 (OriginLab® Corp., Northampton, MA, USA). Significant differences between the various concentrations of AOH/ATXII and the solvent control were assessed by applying the One-way ANOVA followed by Fisher's LSD test. To assess the differences between single treatments and combined treatments, the Student's *t*-test was applied. Differences in intracellular phosphorylation status between the various treatments and the Doxo control (2.5 μM) were evaluated by applying the non-parametric Kruskal-Wallis test followed by the Dunn's multiple comparison test. Significant differences were indicated with * (or $^{\#}$;$p<0.05$), ** ($p<0.01$), and *** ($p<0.001$).

3. Results

3.1. Effects of AOH and ATXII on γH2AX expression and cell viability

The genotoxic effects exerted by AOH (0.1–100 μM) and ATXII (0.1–12.5 μM) on HepG2 cells after 4 h incubation were assessed by applying the γH2AX assay, which allows the indirect detection of DSBs. To avoid misinterpretation of the results due to cytotoxicity, CTB assays were performed in parallel. As shown in Fig. 2, significant increases ($p<0.05$) in γH2AX expression compared to the solvent control (0.5% DMSO) were observed for AOH in the concentration range 10–100 μM. However, such increases were only slight and exposure to 100 μM AOH did not results in a higher γH2AX expression compared to the treatment with 50 μM AOH. Cell viability results showed the ability of AOH to reduce the viability of HepG2 cells starting from a concentration of 50 μM (see supplementary Figure S2). Also in this case, no significant differences in cell viability were observed between treatments with 50 and 100 μM AOH. With respect to the *Alternaria* mycotoxin ATXII, no significant increases in γH2AX expression or reductions in cell viability were observed up to the highest concentration tested (Fig. 2 and supplementary Figure S2).

3.2. Changes in doxorubicin-induced γH2AX expression by the mycotoxin AOH

Based on the results obtained in the γH2AX assay, which showed a slight increase (1.4-fold over the DMSO control) in γH2AX expression following incubation of HepG2 cells with AOH (at 50 μM) and an absence of induction during treatment with ATXII, the hypothesis of a possible inhibition of the kinases involved in the formation of γH2AX by the mycotoxins was formulated. To verify this hypothesis, quantification

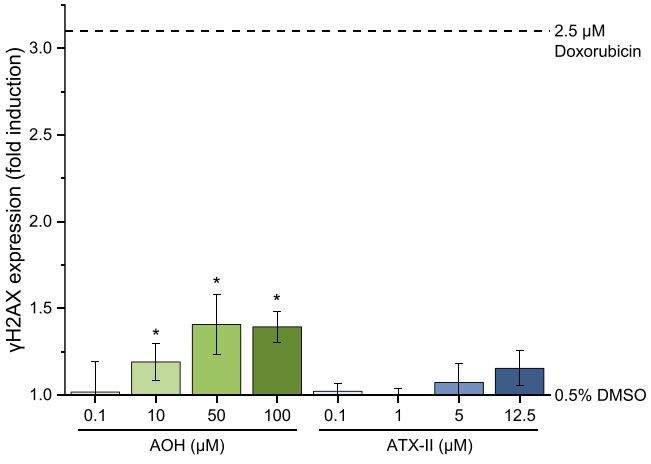

Fig. 2. Effects of the *Alternaria* mycotoxins AOH and ATXII on γH2AX expression. HepG2 cells were exposed to the various concentrations of AOH and ATXII for 4 h. Results were expressed as mean ± SD of at least three biological replicates and normalized to the positive control (2.5 μM Doxo; set as 100%). Differences between the various concentrations of the test compounds and the solvent control were assessed by applying the One-way ANOVA with Fisher's LSD test. * indicates a significant difference ($p<0.05$) compared to the solvent control.

of the phosphorylated histone was performed on HepG2 cells exposed to AOH, Doxo (known to induce DSBs and increase γH2AX expression) or their combinations according to the schema reported in Fig. 1. Fig. 3a shows the γH2AX and CTB results (time points: −1, 0, 2, 4, and 24 h) obtained after single and combined treatments of cells with 5/50 μM AOH and 2.5 μM Doxo (detailed information about the incubation procedure are reported in *Section 2.2* and Fig. 1).

A time-dependent decrease in cell viability was observed after exposure of cells to the various test conditions compared to the DMSO control, except for the single treatment with 5 μM AOH that did not result in any cytotoxic effects even after 24 h incubation. Of note, exposure of cells to 50 μM AOH led to a reduced cell viability (77.0 ± 5.5%) already after 1 h of incubation (timepoint 0 h) and reached the lowest value at timepoint 24 h (36.5 ± 1.6%). Treatment of cells with 2.5 μM Doxo resulted in a reduced cell viability only at timepoint 24 h (65.9 ± 2.2%). A similar reduction (66.4 ± 5.2%) was observed at the same timepoint during co-incubation of Doxo with 5 μM AOH, while exposure of cells to the 2.5 μM Doxo + 50 μM AOH combination led to a reduction in cell viability almost completely overlapping with that induced by 50 μM AOH alone. With respect to the results from the γH2AX assay, Fig. 3a clearly shows the ability of 5 μM AOH to partially suppress ($p<0.05$) the Doxo-induced γH2AX expression at timepoints 4 h and 24 h. Fig. 3b shows representative pictures of cells exposed to 0.5% DMSO, 2.5 μM Doxo, 5 μM AOH, and the combination 2.5 μM Doxo + 5 μM AOH (time point 4 h), in which a slight reduction in γH2AX fluorescence intensity can be observed during the combined treatment. Of note, the reduction in the γH2AX fluorescence signal was even more evident during concomitant treatment of cells with Doxo and 50 μM AOH (compared to Doxo tested alone; Fig. 3a), which resulted in a suppression in fluorescence signal already at timepoint 2 h. These suppressive effects were almost completely overlapping with those induced by 50 μM AOH alone. Interestingly, a slight but significant increase in γH2AX expression was recorded at timepoint 24 h in cells exposed to 50 μM AOH alone (2.17 ± 0.44) as well as in combination with Doxo (2.19

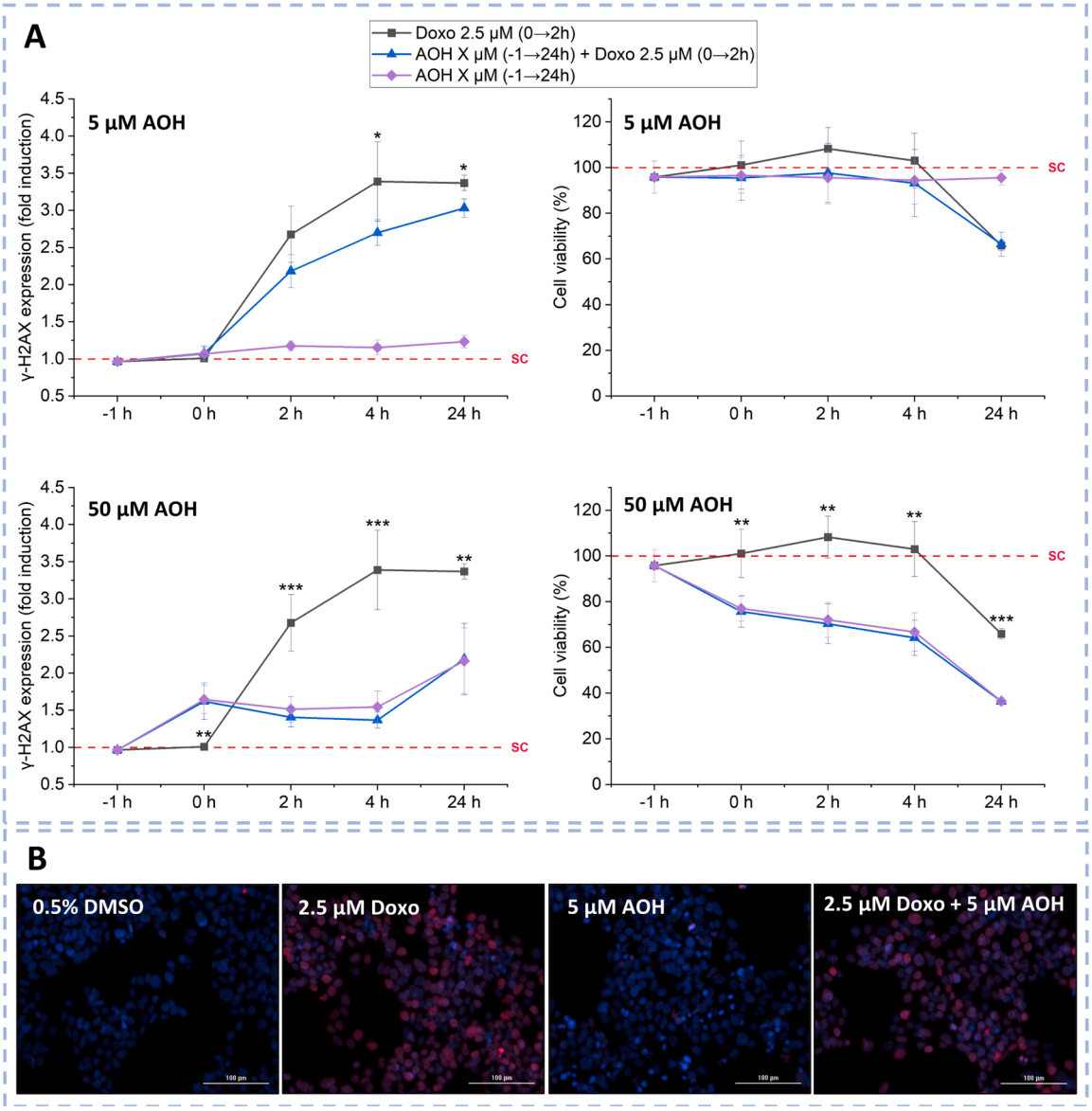

Fig. 3. Impact of AOH on the γH2AX expression induced by the double strand break-inducing compound doxorubicin. A) Line charts reporting the γH2AX and CTB results obtained in HepG2 cells at time points "−1 h, 0 h, 2 h, 4 h, and 24 h" (see Section 2.2 for in-depth information about the incubation conditions). Data are normalized to the solvent control (SC; 0.5% DMSO). B) representative merged images (nucleus: blue; γH2AX: red) of cells exposed to selected test conditions (time point 4 h, scale bars stand for 100μm). Significant differences between the single treatments with Doxo and the respective treatments in combination with AOH were assessed by applying the Student's *t*-test (*$p<0.05$, **$p<0.01$, and ***$p<0.001$).

± 0.48), compared to the timepoints 0, 2, and 4 h.

3.3. Comet assay

To verify whether the reduction in γH2AX expression observed when cells where co-exposed to Doxo and AOH (Fig. 3a) were a consequence of a reduction in DNA damage, the alkaline comet assay was performed at time point 4 h after exposure of cells to 2.5 μM Doxo, 5 μM AOH and their combination. As shown in Fig. 4, whereas treatment with 5 μM AOH did not result in a significant increase in tail intensity compared to the solvent control, exposure of cells to Doxo led to an increase in DNA damage ($p<0.05$). Interestingly, a significantly increase ($p<0.01$) in tail intensity compared to Doxo and AOH as single compounds was observed during the combined treatment. Exposure of cells for 1 min to UV radiation (positive control) resulted in a massive increase ($p<0.001$) in tail intensity, thus confirming the validity of the results obtained.

3.4. In silico analysis

Since the results of the γH2AX expression and the comet assay appeared divergent, we hypothesized that AOH could affect other pathways, potentially influencing the outcomes of these assays in different ways. Along this line, the capability of AOH and ATXII to interfere with the kinases involved in γH2AX formation was verified *in silico*. To do so, it has been calculated the capability of both toxins to interact with the ATP binding site of human serine-protein kinase ATM (UniProt ID Q13315), DNA-PKcs (UniProt ID p78527) and serine/threonine-protein kinase ATR (UniProt ID Q13535), considering the potential of *Alternaria* mycotoxins to compete with ATP previously described (Aichinger et al., 2020). As shown in Fig. 5, both toxins demonstrated a good fit into the ATP binding site of the kinases considered. Indeed, both recorded positive scores (the higher the score, the better the fitting into the pocket; see *Section 2.7* for further details), which pointed to their substantial capability to satisfy the physico-chemical properties of all the pockets analyzed and suitability to arrange in them, though with a slightly different disposition.

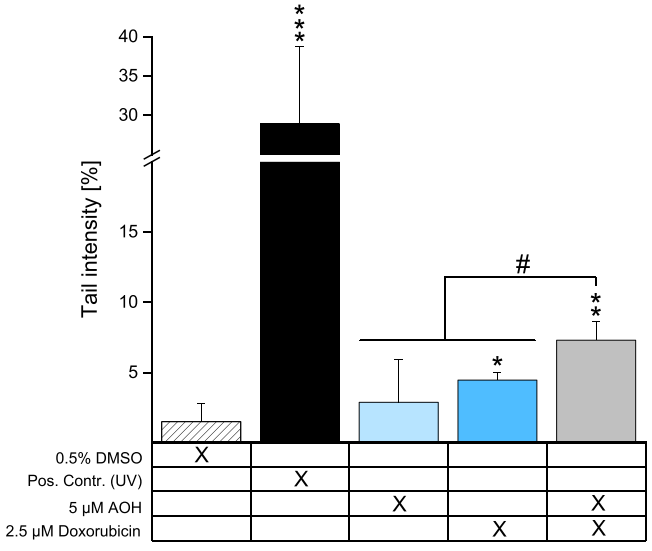

Fig. 4. Results of the comet assay performed on HepG2 cells exposed to AOH and Doxo as single compounds and in combination (timepoint 4 h). Results are expressed as mean ± SD of at least three biological replicates. Student's *t*-test was applied to assess significant differences. *$p<0.05$, **$p<0.01$, ***$p<0.01$ indicate a significant difference compared to the solvent control, while # indicates a significant difference ($p<0.05$) between the co-treatment and the single treatments.

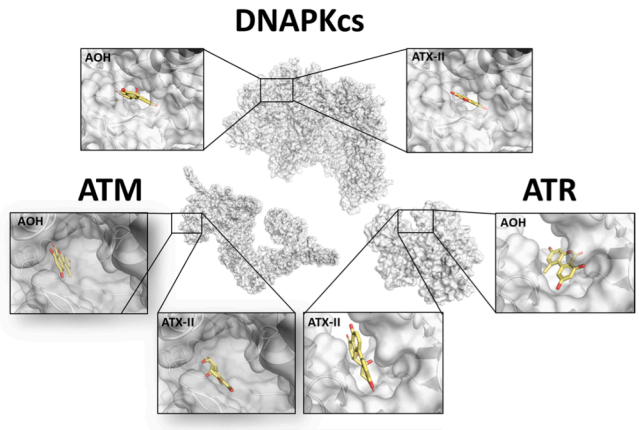

Mycotoxin	Computational scores		
	ATM	ATR	DNAPKcs
AOH	41.5	39.6	62.9
ATX-II	47.5	46.5	65.1

Fig. 5. Docking poses and computational scores of AOH and ATXII.

3.5. Changes in intracellular phosphorylation status during co-treatment of cells with AOH and Doxo

Since *in silico* data inferred for the capacity of AOH and ATXII to modify kinase activity, further analyses were performed to verify if this could be also observed experimentally. Quantification by immunofluorescence of phosphoserine/threonine/tyrosine levels in HepG2 cells exposed to AOH (1, 5, and 10 μM) and Doxo (2.5 μM) as single compounds or in combination was performed to further confirm the hypothesized ability of the mycotoxin to affect the intracellular phosphorylation events. As shown in Fig. 6, exposure of cells to 5 and 10 μM AOH resulted in a reduced ($p<0.05$) nuclear fluorescence intensity compared to Doxo at timepoint 4 h. Similar results were obtained after co-exposure of cells to binary combinations of 5/10 μM AOH and 2.5 μM Doxo. On the contrary, none of the test conditions resulted in changes in intracytoplasmic fluorescence signal compared to Doxo tested alone. With respect to the timepoint 24 h, co-exposure of cells to Doxo and the three concentrations of AOH did not show any change in nuclear and cytoplasmic fluorescence intensities compared to Doxo tested alone, except for the co-treatment "2.5 μM Doxo + 10 μM AOH" which resulted in an increased cytoplasmic fluorescence signal compared to the single treatment with Doxo.

4. Discussion

The emerging *Alternaria* mycotoxin AOH has garnered growing attention from both the scientific community and regulatory bodies due to its frequent presence in food and its potential for a diverse array of toxic effects (Arcella et al., 2016; Crudo et al., 2019; EFSA, 2011). Among the toxicological properties that raise greater concern, genotoxic effects have been reported by several authors (Fleck et al., 2016; Tiessen et al., 2017, 2013). It's worth mentioning that, as per the European Food Safety Authority (EFSA), the consumption of foods with significant AOH contamination might potentially result in exposure levels surpassing the threshold of toxicological concern of 2.5 ng/kg body weight/day (EFSA, 2011). Differently from AOH, very few occurrence and toxicity data are currently available on the epoxide-carrying *Alternaria* mycotoxin ATXII, which was previously reported to exert genotoxic effects and exceeding by far the genotoxic properties of AOH (Fleck et al., 2012; Schwarz et al., 2012). In the present study, the double-strand breaking properties of AOH and ATXII were assessed in the HepG2 cell line (4 h incubation) by quantifying the phosphorylated histone γH2AX, which is formed by members of the family of phosphoinositide 3-kinase-related kinases (PIKKs) following the induction of DSBs (Mah et al., 2010). As shown in Fig. 2, exposure of cells to AOH resulted in a slight but

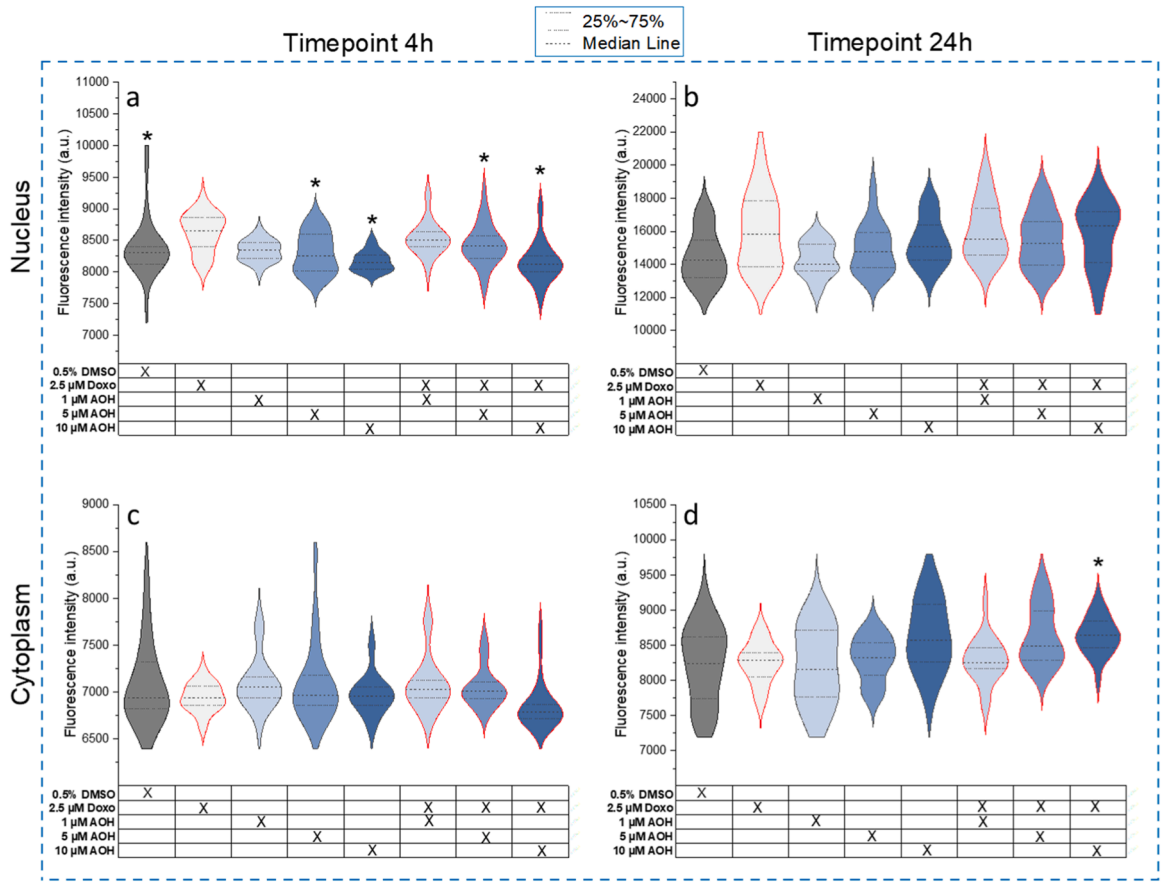

Fig. 6. Quantification by immunofluorescence of phosphoserine/threonine/tyrosine levels in HepG2 cells exposed to AOH and Doxo as single compounds or in combination. a) and b) report the nuclear fluorescence intensity at time points 4 h and 24 h, respectively. c) and d) report the cytoplasmic fluorescence intensity at time points 4 h and 24 h, respectively. Differences between the various treatments and the Doxo control (2.5 µM) were evaluated by applying the Kruskal–Wallis test followed by the Dunn's multiple comparison test. * indicates a significant difference compared to 2.5 µM Doxo ($p < 0.05$).

concentration-dependent increase in γH2AX expression starting from 10 µM. However, exposure to 100 µM AOH did not result in a significant increase in γH2AX formation compared to treatment with 50 µM AOH, suggesting the achievement of a plateau phase. The ability of AOH to induce DSBs was previously reported by Fehr et al., who showed an increase in tail intensity (neutral comet assay) in A431 cells exposed to concentrations of AOH ≥ 10 µM (Fehr et al., 2010). Furthermore, induction of γH2AX by AOH was also reported by Hessel-Pras et al., who found AOH to increase the γH2AX expression in HepG2 cells only at the highest concentration tested (100 µM) (Hessel-Pras et al., 2019). The discrepancy between the results obtained in the present work and those reported by Hessel-Pras et al. could be a consequence of the different detection method used (Hessel-Pras et al., 2019). In fact, while the authors measured the γH2AX expression semi-quantitatively by measuring the absorbance per well followed by normalization to cell viability (MTT assay), in the present study no normalization was performed since the γH2AX fluorescence signal was measured by quantifying the signal per cell nucleus. This approach not only eliminated the necessity for normalization, which would typically be required due to the decreased number of cells, but it also resulted in a noteworthy reduction in data variability across the three biological replicates, as depicted in Fig. 2. Of note, a significant increase in γH2AX expression at concentration of 10 µM was previously reported in V79 cells after 1 h of incubation with the mycotoxin (Fleck et al., 2016). Anyway, the occurrence of DSBs following exposure of cells to AOH likely stemmed from its role as a TOPO poison, particularly targeting the IIα isoform (Fehr et al., 2009). In fact, TOPO II enzyme poisoning causes the persistence of DSBs introduced by the enzyme for DNA topology regulation (Pommier, 2013). Contrary to what was observed for AOH, in the present study the exposure of cells to 0.1–12.5 µM ATXII did not result in any increase in γH2AX expression compared to the solvent control. These findings are in accordance with Fleck et al., who showed the inability of ATXII to enhance the expression of the phosphorylated histone in V79 cells (Fleck et al., 2016). Since AOH and ATXII are known to induce DNA damage, we hypothesized a possible inhibition of the kinases involved in γH2AX formation as a mechanism underlying the limited or lacking ability of AOH and ATXII (respectively) to increase the expression levels of the phosphorylated histone.

To verify this hypothesis, the γH2AX fluorescence signal was quantified in HepG2 cells exposed to binary combinations of 5/50 µM AOH and the DSB-inducing compound Doxo according to the schema reported in Fig. 1. The choice to pre-incubate the cells with AOH prior to addition of the chemotherapeutic drug Doxo was made to allow the mycotoxin to potentially target the kinases before the induction of DSBs by Doxo. After two hours of co-exposure of cells to AOH and Doxo, cells were exposed to the mycotoxin AOH alone in order to evaluate its impact on DNA repair processes. As shown in Fig. 3a, co-treatment with 2.5 µM Doxo and 5 µM AOH resulted in a slight but significant reduction in γH2AX fluorescence signal at timepoints 4 h and 24 h compared to the treatment with 2.5 µM Doxo alone, while co-treatments with 50 µM AOH strongly suppressed the phosphorylation of the histone already at timepoint 2 h. During co-treatment with 5 µM AOH, these suppressions were accompanied by a reduction in cell viability only at time point 24 h. However, this reduced cell viability was a consequence of the cytotoxic effects exerted by Doxo, since the mycotoxin AOH did not affect cell viability when tested alone. It has to be noted that, despite the

cell viability observed during single treatments with Doxo and in combination with 5 μM AOH were almost completely overlapping, a reduced γH2AX expression was observed during the combined treatment compared to the treatment with Doxo alone. This suggests that the reduced γH2AX expression observed during co-treatments was not a consequence of a reduced cell viability but the result of targeting of intracellular processes by AOH. This was even more evident at timepoint 4 h, where a suppression in γH2AX expression was observed in absence of cytotoxic effects. Since the expression levels of γH2AX are known to be strongly affected by the rate of cell proliferation (Seo et al., 2012), the number of cells per optical field found during the execution of the γH2AX assay after exposure to 5 μM AOH and 2.5 μM Doxo (as single compounds and in combination) has been recorded to further exclude the possibility that the observed suppression of γH2AX expression was a consequence of a reduced proliferation rate. As shown in supplementary Figure S1, the proliferation rate was similar in all tested conditions, as a comparable number of cells was present in each acquired picture. Therefore, these results confirm those obtained by applying the CTB assay. Apart for incubations with 5 μM AOH, co-exposure of cells to 2.5 μM Doxo and 50 μM AOH resulted in a more pronounced suppression of γH2AX formation and a more substantial decrease in cell viability. However, the reduction in cell viability during co-treatment with 50 μM AOH were primarily driven by the mycotoxin. Also in this case, although the observed reduction in cell viability might suggest a potential link to the decreased expression of γH2AX observed at the 2 h, 4 h, and 24 h timepoints, an increase in γH2AX expression compared to the earlier measurements was observed at the 24 h timepoint, despite the fact that cell viability had reached its lowest point. Considering that, according to the principle of the γH2AX assay, an increase in γH2AX expression directly correlates with an increase in DSBs (and *vice versa*) (Mah et al., 2010), the results obtained in this study would suggest a reduction in DSBs after co-exposure of cells to Doxo and AOH. However, this appeared highly unlikely given that both compounds are capable of inducing DSBs, primarily by acting as TOPO II poisons (Fehr et al., 2009; van der Zanden et al., 2021).

In order to completely exclude the possible reduction in DNA strand breaks during co-treatment of cells with Doxo and AOH, the alkaline comet assay was performed at time point 4 h in cells exposed to 5 μM AOH and 2.5 μM Doxo as single compounds and in combination. These conditions were chosen because, at this timepoint, reductions in cell viability, which could have potentially led to a misinterpretation of the genotoxicity results, were not observed under any of the tested conditions (Fig. 3a). Differently from the γH2AX assay, the comet assay allows the direct detection of DSBs (neutral comet assay) or the overall DNA damage (SSBs + DSBs; alkaline comet assay) (Collins et al., 2008). In both cases, cell viability must be above 80% to avoid misinterpretation of the results due to cytotoxicity. Based on this, in the present study the execution of the neutral comet assay, which would have allowed for directly comparable results with the γH2AX assay, was hindered by the cytotoxic effects of AOH. Indeed, since DSBs tend to occur at higher concentrations compared to SSBs, using elevated concentrations would have likely induced cytotoxic effects, ultimately rendering the obtained results invalid. Anyway, as shown in Fig. 4, an increase in tail intensity was detected in cells co-exposed to AOH and Doxo compared to the treatment with Doxo alone, thus contradicting the results obtained in the γH2AX assay. Of note, the increased tail intensity was not accompanied by increased cell death, as shown in Fig. 3. This can be explained by the fact that the presence of DNA damage does not necessarily imply the onset of cell death, which actually occurs when the extent of DNA damage is so significant that repair is not possible (Borges et al., 2008; Toyoshima-Sasatani et al., 2023).

Taken together, the results obtained supported the possibility that alternative pathways could be involved downstreaming from the effect of the mycotoxin on the DNA.

To delve deeper into the potential for inhibition of the kinases involved in the γH2AX formation, an *in silico* docking study was conducted to evaluate whether AOH and ATXII could interact with the ATP-binding sites of the three kinases responsible for γH2AX formation, namely ATM, ATR, and DNA-PKc (Mah et al., 2010). Based on docking analysis, both toxins were qualitatively described able to arrange into the ATP binding sites considered, suggesting a certain degree of inhibitory potential due to a competitive binding with ATP. These results might potentially also explain the absence of an increase in γH2AX expression observed after exposure of cells to ATXII, despite its well-known DNA strand break properties (Aichinger et al., 2022; Fleck et al., 2012; Schwarz et al., 2012). However, the low concentrations of the mycotoxin tested and a potentially cell line-specific response might also have contributed to the observed lack of increase in histone expression. Further in-depth studies are required to better explain this discrepancy. Apart for ATXII, the ability of AOH to inhibit the casein kinase 2 (CK2) by interacting with the ATP binding site of the enzyme was previously reported (Aichinger et al., 2020). Therefore, given that ATP-binding sites in kinases are typically highly conserved (Schmidt et al., 2021), there is a reasonable possibility that AOH may not only target CK2 and the kinases involved in γH2AX formation, but also function as a non-specific kinase inhibitor.

Since all previously reported results supported the hypothesis of an inhibition as a mechanism underlying the reduction in γH2AX expression observed, changes in intracellular phosphorylation status were assessed in HepG2 cells exposed to AOH (1, 5, and 10 μM) and Doxo (2.5 μM) as single compounds or in combination. As shown in Fig. 6, the quantification by immunofluorescence microscopy of phosphoserine/threonine/tyrosine levels in the nucleus of cells revealed the ability of the mycotoxin AOH to suppress, at timepoint 4 h, the Doxo-induced increase in intranuclear fluorescence signal at concentrations $\geq$ 5μM. These results further support the hypothesis of an inhibition by AOH of the kinases involved in γH2AX formation. Differently from the timepoint 4 h, no changes in intranuclear phosphorylation status were observed at timepoint 24 h. This is likely a consequence of a reduced availability of the parent compound due to its metabolization in cells. In fact, the mycotoxin AOH was previously reported to be rapidly conjugated with glucuronic acid (AOH-3-O-glucuronide, AOH-9-O-glucuronide) and sulfate (AOH-3-O-sulfat) in differentiated Caco-2 cells (Burkhardt et al., 2009). Furthermore, a recovery of AOH <10% was reported in media of HepG2 cells exposed to the mycotoxin for 24 h (Juan-García et al., 2016). Of note, in the present study, no significant changes in phosphorylation status were observed in the cytoplasm of cells co-exposed to Doxo and AOH at timepoint 4 h, while a significant increase in fluorescence signal was found at timepoint 24 h in cells co-treated with 2.5 μM Doxo and 10 μM AOH compared to Doxo tested alone. Despite more in-depth and dedicated studies are needed to explain the increase in intracytoplasmic phosphorylation phenomena observed, these results are in line with those obtained at the same timepoint in the nucleus, which showed a loss of the inhibitory properties of the mycotoxin after long-term incubation time. Importantly, the data collected in the present study highlight potential difficulties and sources of errors that may occur in the interpretation of a single dataset. This knowledge can support the identification of crucial events to be included in adverse outcome pathways (AOPs) and further strengthen the application of decision trees based on the use of NAMs.

5. Conclusions

This study provides valuable insights into the effects of the *Alternaria* mycotoxins AOH and ATXII on the expression of γH2AX, a crucial player in the cellular response to DNA damage. Notably, AOH slightly induced γH2AX expression, whereas ATXII did not elicit such a response. The observed modest induction of γH2AX by AOH led to the hypothesis that AOH might inhibit the kinases responsible for γH2AX formation. This hypothesis finds support in the data, which demonstrate the ability of AOH to suppress doxorubicin-induced γH2AX expression, despite evidence of increased DNA damage as assessed by the comet assay.

Additionally, a reduction in phosphoserine/threonine/tyrosine levels within the cell nucleus of HepG2 cells during co-exposure to doxorubicin and AOH, compared to doxorubicin alone, was demonstrated. The *in silico* analysis further substantiated this hypothesis, suggesting that AOH could inhibit histone H2AX phosphorylation by competing with ATP for binding to the ATP-binding sites of kinases. However, considering the currently available literature, AOH is more likely to act as a non-selective inhibitor of kinases. Although the limited availability of ATXII constrained *in vitro* experimentation, the absence of a clear increase in γH2AX expression, coupled with the *in silico* findings, indicates the potential of ATXII to inhibit the formation of the γH2AX. It has to be pointed out that, despite the findings of this study suggesting the potential of mycotoxins (especially AOH) to inhibit the kinases responsible for γH2AX formation, it is not possible to completely exclude that other mechanisms might be also involved in the suppressive effects observed. Consequently, more comprehensive and focused studies are essential to precisely elucidate these mechanisms.

This study highlights the imperative of understanding the effects of AOH-induced γH2AX expression inhibition on DNA repair processes, as it is crucial for assessing the risks associated with exposure to this prevalent food contaminant. In fact, even though no carcinogenic properties of AOH have been reported thus far, it is still not possible to exclude that AOH can function as a co-carcinogen by impeding the repair of DNA damages induced by other carcinogens. In addition, the data collected in the present study urgently prompts also an evaluation of the potential of the mycotoxin to interfere with chemotherapy, a critical consideration for cancer treatment strategies. Finally, the study emphasizes the importance of exercising caution when interpreting results from the γH2AX assay, given its growing prominence as a high-throughput genotoxicity assessment tool.

CRediT authorship contribution statement

Doris Marko: Funding acquisition, Methodology, Supervision, Writing – review & editing. **Lena Burger:** Formal analysis, Investigation. **Chenyifan Hong:** Formal analysis, Investigation. **Giorgia Del Favero:** Data curation, Methodology, Writing – review & editing. **Maximilian Jobst:** Formal analysis, Investigation. **Luca Dellafiora:** Data curation, Formal analysis, Investigation, Writing – original draft. **Francesco Crudo:** Conceptualization, Data curation, Formal analysis, Investigation, Methodology, Supervision, Writing – original draft, Writing – review & editing.

Declaration of Competing Interest

The authors declare the following financial interests/personal relationships which may be considered as potential competing interests: Co-author serving as Guest Editor of Toxicology Letters - G.D.F. If there are other authors, they declare that they have no known competing financial interests or personal relationships that could have appeared to influence the work reported in this paper.

Data availability

Data will be made available on request.

Acknowledgements

Microscopy based workflows were supported by the Core Facility Multimodal Imaging of the Faculty of Chemistry of the University of Vienna, member of the VLSI (Vienna Life Science Instruments).

Appendix A. Supporting information

Supplementary data associated with this article can be found in the online version at doi:10.1016/j.toxlet.2024.02.008.

References

Aichinger, G., Dellafiora, L., Pantazi, F., Del Favero, G., Galaverna, G., Dall'Asta, C., Marko, D., 2020. Alternaria toxins as casein kinase 2 inhibitors and possible consequences for estrogenicity: a hybrid in silico/in vitro study. Arch. Toxicol. 94, 2225–2237. https://doi.org/10.1007/s00204-020-02746-x.

Aichinger, G., Grgic, D., Beisl, J., Crudo, F., Warth, B., Varga, E., Marko, D., 2022. N-acetyl cysteine alters the genotoxic and estrogenic properties of Alternaria toxins in naturally occurring mixtures. Emerg. Contam. 8, 30–38. https://doi.org/10.1016/j.emcon.2021.12.004.

Arcella, D., Eskola, M., Gomez Ruiz, J.A., 2016. Dietary exposure assessment to Alternaria toxins in the European population. EFSA J. 14 https://doi.org/10.2903/j.efsa.2016.4654.

Borges, H.L., Linden, R., Wang, J.Y.J., 2008. DNA damage-induced cell death: lessons from the central nervous system. Cell Res 18, 17–26. https://doi.org/10.1038/cr.2007.110.

Burkhardt, B., Pfeiffer, E., Metzler, M., 2009. Absorption and metabolism of the mycotoxins alternariol and alternariol-9-methyl ether in Caco-2 cells in vitro. Mycotoxin Res 25, 149–157. https://doi.org/10.1007/s12550-009-0022-2.

Burley, S.K., Bhikadiya, C., Bi, C., Bittrich, S., Chao, H., Chen, L., Craig, P.A., Crichlow, G. V., Dalenberg, K., Duarte, J.M., Dutta, S., Fayazi, M., Feng, Z., Flatt, J.W., Ganesan, S., Ghosh, S., Goodsell, D.S., Green, R.K., Guranovic, V., Henry, J., Hudson, B.P., Khokhriakov, I., Lawson, C.L., Liang, Y., Lowe, R., Peisach, E., Persikova, I., Piehl, D.W., Rose, Y., Sali, A., Segura, J., Sekharan, M., Shao, C., Vallat, B., Voigt, M., Webb, B., Westbrook, J.D., Whetstone, S., Young, J.Y., Zalevsky, A., Zardecki, C., 2023. RCSB Protein Data Bank (RCSB.org): delivery of experimentally-determined PDB structures alongside one million computed structure models of proteins from artificial intelligence/machine learning. Nucleic Acids Res 51, D488–D508. https://doi.org/10.1093/nar/gkac1077.

Cattaneo, I., Astuto, M.C., Binaglia, M., Devos, Y., Dorne, J.L.C.M., Fernandez Agudo, A., Fernandez Dumont, A., Garcia-Vello, P., Kass, G.E.N., Lanzoni, A., Liem, A.K.D., Panzarea, M., Paraskevopulos, K., Parra Morte, J.M., Tarazona, J.V., Terron, A., 2023. Implementing new approach methodologies (NAMs) in food safety assessments: strategic objectives and actions taken by the European Food Safety Authority. Trends Food Sci. Technol. 133, 277–290. https://doi.org/10.1016/j.tifs.2023.02.006.

Chen, S., Lee, L., Naila, T., Fishbain, S., Wang, A., Tomkinson, A.E., Lees-Miller, S.P., He, Y., 2021. Structural basis of long-range to short-range synaptic transition in NHEJ. Nature 593, 294–298. https://doi.org/10.1038/s41586-021-03458-7.

Cohen-Khait, R., Dym, O., Hamer-Rogotner, S., Schreiber, G., 2017. Promiscuous protein binding as a function of protein stability. Structure 25, 1867–1874.e3. https://doi.org/10.1016/j.str.2017.11.002.

Collins, A.R., 2004. The comet assay for DNA damage and repair: principles, applications, and limitations. Appl. Biochem. Biotechnol. Part B Mol. Biotechnol. 26, 249–261. https://doi.org/10.1385/MB:26:3:249.

Collins, A.R., Oscoz, A.A., Brunborg, G., Gaivão, I., Giovannelli, L., Kruszewski, M., Smith, C.C., Štětina, R., 2008. The comet assay: topical issues. Mutagenesis 23, 143–151. https://doi.org/10.1093/mutage/gem051.

Crudo, F., Varga, E., Aichinger, G., Galaverna, G., Marko, D., Dall'Asta, C., Dellafiora, L., 2019. Co-occurrence and combinatory effects of alternaria mycotoxins and other xenobiotics of food origin: current scenario and future perspectives. Toxins (Basel) 11, 1–29. https://doi.org/10.3390/toxins11110640.

Crudo, F., Aichinger, G., Dellafiora, L., Kiss, E., Mihajlovic, J., Del Favero, G., Berry, D., Dall'Asta, C., Marko, D., 2022. Persistence of the antagonistic effects of a natural mixture of Alternaria mycotoxins on the estrogen-like activity of human feces after anaerobic incubation. Toxicol. Lett. 358, 88–99. https://doi.org/10.1016/j.toxlet.2022.01.015.

Crudo, F., Hong, C., Varga, E., Del Favero, G., Marko, D., 2023. Genotoxic and mutagenic effects of the alternaria mycotoxin alternariol in combination with the process contaminant acrylamide. Toxins 15. https://doi.org/10.3390/toxins15120670.

van der Zanden, S.Y., Qiao, X., Neefjes, J., 2021. New insights into the activities and toxicities of the old anticancer drug doxorubicin. FEBS J. 288, 6095–6111. https://doi.org/10.1111/febs.15583.

Ebmeyer, J., Braeuning, A., Glatt, H., These, A., Hessel-Pras, S., Lampen, A., 2019. Human CYP3A4-mediated toxification of the pyrrolizidine alkaloid lasiocarpine. Food Chem. Toxicol. 130, 79–88. https://doi.org/10.1016/j.fct.2019.05.019.

EFSA, 2011. Scientific Opinion on the risks for animal and public health related to the presence of Alternaria toxins in feed and food. EFSA J. 9, 1–97. https://doi.org/10.2903/j.efsa.2011.2407.

Fehr, M., Pahlke, G., Fritz, J., Christensen, M.O., Boege, F., Altemöller, M., Podlech, J., Marko, D., 2009. Alternariol acts as a topoisomerase poison, preferentially affecting the IIα isoform. Mol. Nutr. Food Res 53, 441–451. https://doi.org/10.1002/mnfr.200700379.

Fehr, M., Baechler, S., Kropat, C., Mielke, C., Boege, F., Pahlke, G., Marko, D., 2010. Repair of DNA damage induced by the mycotoxin alternariol involves tyrosyl-DNA phosphodiesterase 1. Mycotoxin Res 26, 247–256. https://doi.org/10.1007/s12550-010-0063-6.

Fernández-Blanco, C., Font, G., Ruiz, M.J., 2015. Oxidative DNA damage and disturbance of antioxidant capacity by alternariol in Caco-2 cells. Toxicol. Lett. 235, 61–66. https://doi.org/10.1016/j.toxlet.2015.03.013.

Fleck, S.C., Burkhardt, B., Pfeiffer, E., Metzler, M., 2012. Alternaria toxins: Altertoxin II is a much stronger mutagen and DNA strand breaking mycotoxin than alternariol and its methyl ether in cultured mammalian cells. Toxicol. Lett. 214, 27–32. https://doi.org/10.1016/j.toxlet.2012.08.003.

Fleck, S.C., Sauter, F., Pfeiffer, E., Metzler, M., Hartwig, A., Köberle, B., 2016. DNA damage and repair kinetics of the Alternaria mycotoxins alternariol, altertoxin II and

stemphyltoxin III in cultured cells. Mutat. Res. Genet Toxicol. Environ. Mutagen 798–799, 27–34. https://doi.org/10.1016/j.mrgentox.2016.02.001.
Hessel-Pras, S., Kieshauer, J., Roenn, G., Luckert, C., Braeuning, A., Lampen, A., 2019. In vitro characterization of hepatic toxicity of Alternaria toxins. Mycotoxin Res. 35, 157–168. https://doi.org/10.1007/s12550-018-0339-9.
Jobst, M., Kiss, E., Gerner, C., Marko, D., Del Favero, G., 2023. Activation of autophagy triggers mitochondrial loss and changes acetylation profile relevant for mechanotransduction in bladder cancer cells. Arch. Toxicol. 97, 217–233. https://doi.org/10.1007/s00204-022-03375-2.
Juan-García, A., Juan, C., Manyes, L., Ruiz, M.J., 2016. Binary and tertiary combination of alternariol, 3-acetyl-deoxynivalenol and 15-acetyl-deoxynivalenol on HepG2 cells: toxic effects and evaluation of degradation products. Toxicol. Vitr. 34, 264–273. https://doi.org/10.1016/j.tiv.2016.04.016.
Kopp, B., Khoury, L., Audebert, M., 2019. Validation of the γH2AX biomarker for genotoxicity assessment: a review. Arch. Toxicol. https://doi.org/10.1007/s00204-019-02511-9.
Mah, L.J., El-Osta, A., Karagiannis, T.C., 2010. γh2AX: a sensitive molecular marker of DNA damage and repair. Leukemia 24, 679–686. https://doi.org/10.1038/leu.2010.6.
Maldonado-Rojas, W., Olivero-Verbel, J., 2011. Potential interaction of natural dietary bioactive compounds with COX-2. J. Mol. Graph Model 30, 157–166. https://doi.org/10.1016/j.jmgm.2011.07.002.
Mikušová, P., Sulyok, M., Šrobárová, A., 2014. Alternaria mycotoxins associated with grape berries in vitro and in situ. Biologia 69, 173–177. https://doi.org/10.2478/s11756-013-0306-z.
Pommier, Y., 2013. Drugging topoisomerases: lessons and challenges Yves. ACS Chem. Biol. 8, 82–95. https://doi.org/10.1021/cb300648v.
Puntscher, H., Hankele, S., Tillmann, K., Attakpah, E., Braun, D., Kütt, M.L., Del Favero, G., Aichinger, G., Pahlke, G., Höger, H., Marko, D., Warth, B., 2019. First insights into Alternaria multi-toxin in vivo metabolism. Toxicol. Lett. 301, 168–178. https://doi.org/10.1016/j.toxlet.2018.10.006.
Puntscher, H., Marko, D., Warth, B., 2020. First determination of the highly genotoxic fungal contaminant altertoxin II in a naturally infested apple sample. Emerg. Contam. 6, 82–86. https://doi.org/10.1016/j.emcon.2020.01.002.
Rao, Q., Liu, M., Tian, Y., Wu, Z., Hao, Y., Song, L., Qin, Z., Ding, C., Wang, H.W., Wang, J., Xu, Y., 2018. Cryo-EM structure of human ATR-ATRIP complex. Cell Res 28, 143–156. https://doi.org/10.1038/cr.2017.158.
Schmidt, D., Scharf, M.M., Sydow, D., Aßmann, E., Martí-Solano, M., Keul, M., Volkamer, A., Kolb, P., 2021. Analyzing kinase similarity in small molecule and protein structural space to explore the limits of multi-target screening. Molecules 26, 1–19. https://doi.org/10.3390/molecules26030629.
Schrader, T.J., Cherry, W., Soper, K., Langlois, I., Vijay, H.M., 2001. Examination of Alternaria alternata mutagenicity and effects of nitrosylation using the ames Salmonella test. Teratog. Carcinog. Mutagen 21, 261–274. https://doi.org/10.1002/tcm.1014.
Schwarz, C., Tiessen, C., Kreutzer, M., Stark, T., Hofmann, T., Marko, D., 2012. Characterization of a genotoxic impact compound in Alternaria alternata infested rice as altertoxin II. Arch. Toxicol. 86, 1911–1925. https://doi.org/10.1007/s00204-012-0958-4.
Seo, J., Kim, S.C., Lee, H.S., Kim, J.K., Shon, H.J., Salleh, N.L.M., Desai, K.V., Lee, J.H., Kang, E.S., Kim, J.S., Choi, J.K., 2012. Genome-wide profiles of H2AX and γ-H2AX differentiate endogenous and exogenous DNA damage hotspots in human cells. Nucleic Acids Res 40, 5965–5974. https://doi.org/10.1093/nar/gks287.
Solhaug, A., Vines, L.L., Ivanova, L., Spilsberg, B., Holme, J.A., Pestkab, J., Collins, A., Eriksen, G.S., 2012. Mechanisms involved in alternariol-induced cell cycle arrest. Mutat. Res. - Fundam. Mol. Mech. Mutagen. 738–739, 1–11. https://doi.org/10.1016/j.mrfmmm.2012.09.001.
Soukup, S.T., Fleck, S.C., Pfeiffer, E., Podlech, J., Kulling, S.E., Metzler, M., 2020. DNA reactivity of altertoxin II: Identification of two covalent guanine adducts formed under cell-free conditions. Toxicol. Lett. 331, 75–81. https://doi.org/10.1016/j.toxlet.2020.05.018.
Tiessen, C., Gehrke, H., Kropat, C., Schwarz, C., Bächler, S., Fehr, M., Pahlke, G., Marko, D., 2013. Role of topoisomerase inhibition and DNA repair mechanisms in the genotoxicity of alternariol and altertoxin-II. World Mycotoxin J. 6, 233–244. https://doi.org/10.3920/wmj2013.1592.
Tiessen, C., Ellmer, D., Mikula, H., Pahlke, G., Warth, B., Gehrke, H., Zimmermann, K., Heiss, E., Fröhlich, J., Marko, D., 2017. Impact of phase I metabolism on uptake, oxidative stress and genotoxicity of the emerging mycotoxin alternariol and its monomethyl ether in esophageal cells. Arch. Toxicol. 91, 1213–1226. https://doi.org/10.1007/s00204-016-1801-0.
Toyoshima-Sasatani, M., Imura, F., Hamatake, Y., Fukunaga, A., Negishi, T., 2023. Mutation and apoptosis are well-coordinated for protecting against DNA damage-inducing toxicity in Drosophila. Genes Environ. 45 https://doi.org/10.1186/s41021-023-00267-4.
Tice, R.R., Agurell, E., Anderson, D., Burlinson, B., Hartmann, A., Kobayashi, H., Miyamae, Y., Rojas, E., Ryu, C., Sasaki, Y.F., 2000. Single cell gel/comet assay: Guidelines for in vitro and in vivo genetic toxicology testing. Environ Mol Mutagen 35 (3), 206–221. https://doi.org/10.1002/(SICI)1098-2280(2000)35:33.0.CO;2-J.
Wahyuni, E.A., Yii, C.Y., Liang, H.L., Luo, Y.H., Yang, S.H., Wu, P.Y., Hsu, W.L., Nien, C. Y., Chen, S.C., 2022. Selenocystine induces oxidative-mediated DNA damage via impairing homologous recombination repair of DNA double-strand breaks in human hepatoma cells. Chem. Biol. Inter. 365 https://doi.org/10.1016/j.cbi.2022.110046.